Sensor Letters

Electroless Au Plating of CMOS Microelectrodes: Fabrication, Characterisation and Electrochemical Measurement

Minghao Li[1,2*], Aishath N. Naeem[2*], Henry T. Lancashire[3**], Anne Vanhoestenberghe[4**], and Sara S. Ghoreishizadeh[2***]

[1]*Division of Surgery and Interventional Sciences;* [2]*Dept. of Electrical and Electronics Eng.;* [3]*Dept. of Medical Physics and Biomedical Eng., University College London.* [4]*School of Biomedical Engineering and Imaging Sciences, King's College London, London, UK*
[*]*Student Member, IEEE,* [**]*Member, IEEE,* [***]*Senior Member, IEEE*

Abstract—An essential step in developing amperometric sensors directly on CMOS integrated circuits (ICs) is to cover the exposed uppermost metal layer (aluminium pads) with a thin layer of noble metal to form the basis of the sensing electrode. A simple and scalable method to achieve the gold layer is through electroless plating. Despite the popularity of electroless plating in e.g. PCB manufacturing, there is a lack of information on how it can be applied to Al microelectrodes, and what the electrochemical performances of Au-coated microelectrodes are. This paper presents a detailed process for electroless gold plating of CMOS microelectrodes, with a step-by-step characterisation of the surface roughness, thickness, and elemental composition to optimise the deposition parameters (e.g. deposition time and temperature) for achieving a smooth and uniform gold coverage of the microelectrodes. A gold layer with a rms surface roughness of 53.6±7.9 nm is achieved on the microelectrodes and successfully characterised by cyclic voltammetry in a ferri/ferrocyanide solution. Sonication, oxygen plasma, and continuous cyclic voltammetry are applied to the Au-coated microelectrodes to determine their mechanical and electrochemical stability.

Index Terms—Microelectrodes, CMOS chip, electroless gold plating, surface topography, electrode characterization.

I. INTRODUCTION

The monolithic integration of electrochemical sensors and readout electronics on semiconductor (e.g. CMOS) technology provides scalability while improving the signal-to-noise ratio of measurements [1], [2]. The integration provides several other advantages such as low-cost sensor redundancy and multi-target detection through embedding large sensor arrays on a single device. It also allows miniaturisation of sensors, which in turn enables the use of low sample volumes. There are several examples of commercially available CMOS integrated sensor arrays for applications in optical imaging or DNA analysis [3][4][5] where a direct charge transfer to the sensor is not required for its operation.

A wide range of biomolecule sensors do require charge transfer between the sensing electrode and the electrolyte (sample biofluid). Examples include redox-based and nanopore-based sensors where a conductive sensing electrode needs to be placed in direct contact with the (bio)fluid to allow the transfer or induction of charge [6]. To integrate such sensors on CMOS, the exposed top metal layer (the pads) can be used as the base. However, this layer is typically nearly pure aluminium (Al) which is an electroactive material unsuitable for electrochemical sensing [7]. The first essential step in sensor development is to cover this layer with an appropriate metal film.

Gold (Au) is widely used as the electrode surface material in electrochemical measurements due to its bio-compatibility, high conductivity, and low ionization tendency in the transition metal series (i.e. being inert) [8]. There are several techniques for depositing a gold layer on dissimilar metallic surfaces. A few have been applied to CMOS Al microelectrodes as well. These are physical vapour deposition (e.g. sputtering) [9], Au bumping (use of ball wire bonder to leave a bump of gold on the pad) [10], electroless gold deposition (that is chemical deposition of Au from a suitable solution onto the surfaces) [11], and electroplating (that is electrochemical deposition of gold from a suitable solution onto the surface) [12].

Electroless plating is by far the simplest, least expensive, and most scalable technique as it does not require any cleanroom-based equipment (unlike PVD), nor any electrical connection to the electrode (unlike electroplating), or individual handling of the electrodes (unlike gold bumping). However, despite widespread usage in the PCB and jewellery industries, and its demonstration in CMOS microelectrodes [11], [13], [14], there is a gap in the literature; the required steps and parameters to achieve a smooth and uniform Au layer (two common prerequisites for most biological sensors [15]) on CMOS Al microelectrodes are not yet known, and the performance and stability of such Au-coated electrodes for electrochemical sensing have not been reported yet.

In this work, we present a detailed electroless plating procedure along with optimised parameters to achieve a uniform and smooth Au film on *CMOS Al microelectrodes* (CAlm). The microelectrodes are characterised at each step using imaging techniques, and their utility for electrochemical sensing is demonstrated through cyclic voltammetry characterisation in a ferri/ferrocyanide solution.

II. MATERIALS AND METHODS

1) Materials: Bright Au electroless plating solution, sodium hydroxide, and potassium ferri/ferrocyanide were purchased from Sigmal Aldrich. Xenolyte zincate CFA was purchased from Atotech. Nitric acid (Honeywell), phosphate buffer solution (PBS), acetone, isopropanol alcohol (IPA), and de-ionised (DI) water were also used. Nickel electroless plating solution was prepared by mixing 1 mL nickel sulfate hexahydrate (28 g/L in DI water, from Sigma) and 1 mL sodium hypophosphite (27 g/L in DI water, from Sigma). Silver conductive epoxy (8331D) was purchased from MG Chemicals. An epoxy (EP41S-5) from Masterbond was used to protect the wires.

Authors email addresses: {minghao.li.19, aishath.naeem, h.lancashire, s.ghoreishizadeh}@ucl.ac.uk; a.vanhoest@kcl.ac.uk
Digital Object Identifier 10.1109/LSENS.2017.0000000

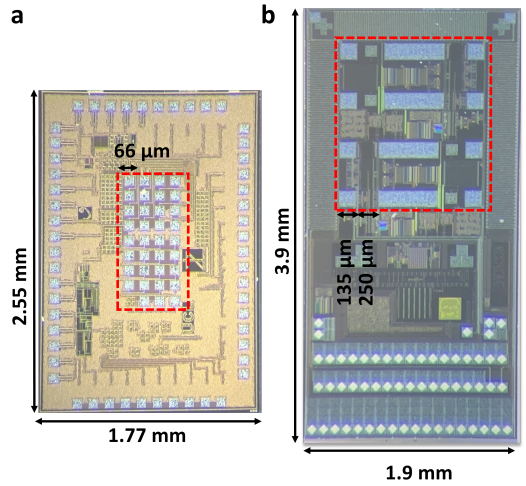

Fig. 1. Microphotograph of (a) CMOS chip no.1, fabricated in TSMC 180 nm and (b) CMOS chip no.2 fabricated in AMS 350 nm, showing Al micro-electrodes in the middle of the chips (not in the same scale).

2) Equipment: Scanning electron microscopy (SEM) and energy dispersive X-ray (EDX) were carried out using a JEOL IT100 SEM for surface morphology and composition analysis. Atomic force microscopy (AFM) was carried out using a NaioAFM (Nanosurf) for surface roughness and thickness measurements. A focused ion beam (NV40, Zeiss) was used to measure the thickness of Au film. A potentiostat (Autolab, Metrohm) was used for electrochemical characterisation and measurements. A semi-automatic wire-bonding machine (F & S Bondtec 5632) with 25 µm thick Au wires was used to connect the chip pads to a carrier PCB. An oven (ED056, Binder) and an ultrasound cleaner (VWR) were also used.

3) CMOS microelectrode fabrication: CMOS chips designed separately using different CMOS technology nodes and manufacturers (see Fig. 1) were used. (i) Chip no. 1 was designed in 180 nm CMOS technology, and fabricated by Taiwan Semiconductor Manufacturing Company, TSMC. The chip has an array of 32 microelectrodes of 66 μm × 66 μm with an edge-to-edge spacing of 40 μm. Two of these microelectrodes are also directly accessible from outside the chip and were therefore used for electrochemical characterisation and measurement using the bench-top potentiostats mentioned above. (ii) Chip no. 2 was designed in 350 nm CMOS technology, and fabricated by AMS Osram AG, AMS. The chip has an array of Al microelectrodes with the smallest (135 μm × 135 μm) used in this work to optimise the deposition steps and characterisation using SEM and EDX. There is a 99.6% Al in the microelectrodes of both chips. The average roughness of Al microelectrodes was measured to be 23 nm rms, and 28 nm rms for chips no.1 and no.2, respectively.

III. ELECTROLESS AU DEPOSITION ON CMOS MICROELECTRODES

The direct deposition of Au films over Al is not recommended due to the poor adhesion of Au to Al. An adhesive interlayer such as Ni is typically used prior to Au deposition [16] due to its good adhesion to Au. However, Al lacks an inner vacant electron orbit which is generally needed for the auto-catalytic electroless Ni deposition [17]. An activation layer typically in Zn (due to the simplicity of zincation [18]) is therefore required prior to Ni deposition. The Zn layer also protects and prevents Al from re-oxidation. The electroless Au deposition process developed in this work is therefore based on the sequential electroless deposition of Zn, Ni, and Au layers from their respective solutions onto the microelectrode surface.

The Au plating step is a displacement process where Ni atoms are replaced with Au atoms. It is therefore suggested that the thickness of the Au film depends on the thickness of the Ni film [14].

The main parameter that has been optimised in this work is the deposition time for each of Zn, Ni, and Au, in order to achieve a smooth and uniform surface (as confirmed through imaging) as well as an electrochemically stable surface (as confirmed through cyclic voltammetry tests).

1) Surface cleaning: The process starts with the preparation of the chip through surface cleaning and Al oxide removal. The chip is placed in a glass beaker filled with acetone and IPA in order at room temperature. The glass beaker is then placed in an ultrasound bath for 1 minute to remove organic contaminants and dust from the surface. After that, the chip is rinsed with DI water.

Following the cleaning step, the chip is etched slightly to remove Al oxide from the CAlm and expose Al. The chip is dipped in a beaker containing 10% sodium hydroxide (NaOH) in DI water for a duration of 2 minutes at room temperature. The chip is rinsed with nitric acid (HNO_3) for a few seconds to remove residual sodium hydroxide and clean the surface ahead of the zincate process.

2) Electroless Zn deposition: During the zincate process, a thin layer of Al is replaced with zinc. A double zincate process (rather than single zincate) was chosen to achieve a more uniform and dense Zn layer without any large Zn grains in order to improve adhesion of Ni film at the next stage [13].

Each single zincate step was carried out by dipping the chip inside a beaker containing 0.5 mL of Zn electroless plating solution for 1 minute [18] at either room temperature or 45 °C [11]. After the first zincate, the chip was immersed in a beaker with 20% nitric acid at room temperature for 45 seconds, before the second zincate process.

The surface morphology after the double zincate process at 45 °C is shown in Fig. 2. (a) where a smooth surface with small Zn grains can be observed. The surface composition analysis (at the same deposition temperature) confirms a Zn percentage close to 10 wt% which is large enough for a good Ni adhesion [18]. Deposition at room temperature led to a much smaller Zn percentage of around 2%. It should be noted that the EDX setup used (accelerating voltage of 15 kV) is capable of examining the top 0.5 µm thickness of the microelectrode surface therefore observing a large percentage of Al in post-zincate EDX graphs is expected.

A typical defect observed at this point was the formation of large Zn grains which would cause high roughness in the final gold layer. This was found to be dependent on the temperature at which the chip was held during the zincation process and the concentration of the zincation solution. To resolve this, the chip was placed in an oven (instead of using a hot plate) to ensure equal temperatures throughout the chip and zincation solution and the full concentration of the zincation solution was used.

3) Electroless Ni deposition: A Ni-P-based deposition was chosen over a pure Ni deposition as it is known to achieve a smoother Ni film with smaller nucleation sites [11], [19]. The chip was dipped in 1 ml of Ni electroless plating solution. The deposition time was varied from 10 to 40 minutes. The deposition temperature was kept at 85 °C [20] using an oven.

The surface morphology analysis after Ni-P deposition indicates increasing Ni cluster size with increased deposition time from 10

to 25 minutes. At 25 minutes, a complete coating with Ni-P film is achieved. However, increasing the time beyond 25 minutes leads to increased grain size and a rougher surface overall (shown in Fig. 2 (b)). The surface composition analysis shows a 90% Ni after 25 minutes of Ni-P deposition, confirming that 25 minutes is the optimum time. The remaining 10% is P.

4) Electroless Au deposition: The Au plating on Ni-coated microelectrodes was carried out by dipping the chip in a beaker with 1 mL of Au electroless solution for 15 minutes or 30 minutes. The temperature was kept at 90 °C (per supplier recommendations) during the deposition time by placing the beaker with the chip inside an oven. The formation of a dense and uniform gold layer was confirmed using SEM (see Fig. 2 (c)). The peaks observed in the surface composition analysis confirm that the first around 0.5 μm thickness is 97% Au after 15 minutes of Au deposition.

The surface roughness of Zn, Ni and Au-coated electrodes on five different chips was measured using SEM and summarised in Table 1, along with elemental composition and the optimised deposition parameters. The deposition of each layer improves the smoothness of the surface. The average roughness (measured on three electrodes) at the surface of Au film is 53.8 ± 7.9 nm rms after 15 minutes of Au deposition. A 30-minute deposition leads to a higher roughness without changing the film thickness and thus 15 minutes was deemed more suitable.

5) thickness characterisation: The thickness of Zn and Ni layers were calculated by taking the difference between the heights of the microelectrode and the top CMOS passivation, before and after the deposition of a layer using the AFM. The average thickness of three microelectrodes of Zn and Ni films measured on three electrodes are 123 ± 7 nm and 692 ± 45 nm, respectively.

The Au layer thickness was measured using FIB, by making a 2 μm deep hole in the middle of the Au-coated microelectrode and observing the cross-section of the electrode. The average thickness of Au on two electrodes was measured to be 545 nm and 509 nm. All thickness analysis and following electrochemical tests were carried out using microelectrodes on chip no. 1.

IV. ELECTROCHEMICAL MEASUREMENTS

1) Wirebonding and encapsulation: After the completion of the electroless Au deposition process, the chip was glued to a carrier PCB using silver conductive epoxy, and the peripheral pads were electrically connected to PCB pads using Au bond wires. The wires were then encapsulated using non-conductive epoxy to protect them and leave the microelectrodes in the middle of the chip exposed. The epoxy was left to cure overnight. A plastic or a glass ring was glued on the PCB on top of the chip using the non-conductive epoxy, to form a reservoir to contain the sample fluid during electrochemical measurements. An illustration of this is shown in Fig. 3 (a).

2) Cyclic voltammetry in potassium ferri/ferrocyanide: The Au-plated microelectrode was used as a working electrode in a three-electrode setup with an off-chip Ag|AgCl electrode as the reference (RE) and a platinized titanium electrode as the counter electrode (CE). The RE and CE were placed inside the reservoir close to the WE and the reservoir was filled with test solutions. Cyclic Voltammetry measurements were carried out (at 0 mV to 400 mV with a scan rate of 100 mV/s) in PBS, and again in the presence of potassium ferrocyanide and potassium ferricyanide with equal concentrations of 1.25 mM, 2.5 mM, and 5 mM in PBS. The voltammograms acquired using two different microelectrodes are shown in Fig. 3. (b). The position and amplitude of the peaks and the overall shape of the voltammogram are as expected for ferri/ferro redox reaction [14]. The peak current versus concentration of ferri/ferrocyanide (presented in Fig. 3. (c)) demonstrates a good linearity with R^2 of 0.994.

TABLE 1. Optimised parameters with mean and standard deviation for electroless Zn, Ni and Au deposition on CAlm, and measured surface roughness and elemental composition. All measurements carried out on five chips (CMOS chip no. 2).

Metal	Deposition time (min)	Deposition temperature (℃)	Surface roughness (nm)	Elemental composition (%)
Al	-	-	28.4 ± 0.3	99.6 ± 0.1
Zn	2	45	125.7 ± 16.2	10.22 ± 1.56
Ni	25	85	72.3 ± 7.6	89.20 ± 0.51
Au	15	90	53.8 ± 7.9	97.15 ± 1.06

3) Fabrication yield and electrode stability: The optimised parameters shown in Table 1 were used for electroless Au plating on over 30 chips and no plating defects were detected when examined under the optical microscope. The chips were then used for various biosensing purposes.

The electrochemical stability of three Au-coated microelectrodes on three different chips was examined by continuous cyclic voltammetry (between -0.2 V and 0.4 V with a scan rate of 100 mV/s) in PBS (pH=7.4). The electrodes were stable for the first 2±1 cycles and then started showing signs of instability, as shown in Fig. 3(d). There were no signs of physical change (e.g. peeling off) on the surface of these electrodes. The electrodes underwent sonication in DI water (at 45 kHz) for two minutes, which did not help in reviving the electrodes electrochemically. The electrodes still did not show any sign of physical degradation when examined under SEM after the sonication. The electrodes then underwent oxygen plasma cleaning for five minutes, after which it was observed that the Au film was partially peeled off. It can be concluded that the electrodes are more suitable for a single-time measurement as statistics obtained using three electrodes show that instability can appear only after a few CV cycles. The electrochemical instability is likely to be due to chloride ion adsorption [21]. This could potentially be resolved through surface cleaning with oxygen plasma for a thicker Au layer.

V. CONCLUSION

In this paper, a step-by-step process is presented for electroless Au deposition on CMOS Al microelectrodes. We show that with careful control of the duration and temperature during the Zn, Ni and Au plating, as well as the individual choice of plating solution (e.g. Ni/P over Ni, double zincation) a smooth Au film with roughness as low as 53 nm rms can be obtained. The gold-covered CMOS microelectrode shows the typical voltammogram response of a gold macro electrode in the presence of ferri/ferrocyanide. Although stable after sonication, the Au layer peels off when undergoing oxygen plasma for 5 minutes and shows signs of instability after (on average) two cycles of cyclic voltammetry.

ACKNOWLEDGMENT

The authors would like to thank Dr. Atal A. Gill for his initial works on zincate and Ni plating. SG thanks Prof Pantelis Georgious for his support in design and fabrication of chip no. 2. For the purpose of open access, the author has applied a Creative Commons

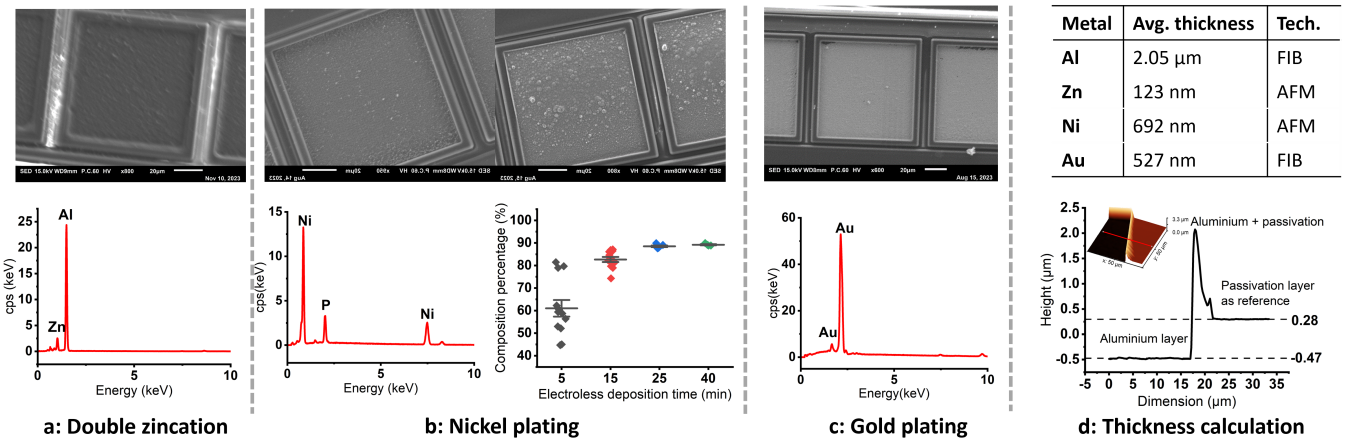

Metal	Avg. thickness	Tech.
Al	2.05 μm	FIB
Zn	123 nm	AFM
Ni	692 nm	AFM
Au	527 nm	FIB

Fig. 2. SEM images and EDX spectrum of microelectrodes (on CMOS die no. 2) taken after (a) double zincation, (b) nickel plating: SEM images taken after 25 and 40 minutes; EDx after 25 minutes and composition percentage of nickel vs different plating time, and (c) gold plating for 15 minutes. (d) The thickness of each layer measured immediately after each deposition using AFM or FIB; and an example of AFM image used as a reference for calculating deposited Zn and Ni film thicknesses. The peak shown in AFM image indicates the boundary of the microelectrodes).

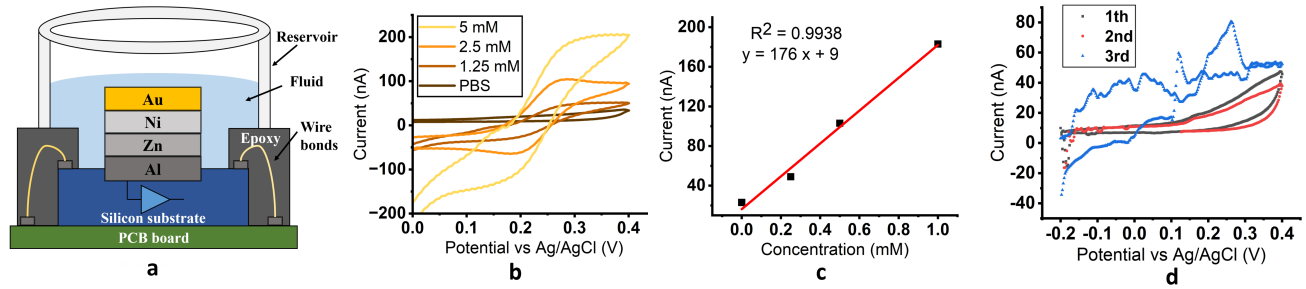

Fig. 3. (a) An illustration of various layers deposited on the CMOS Al microelectrode and the chip preparation for electrochemical testing. (b) Cyclic voltammetry measurement with Au-coated CMOS microelectrodes in various ferri/ferrocyanide concentrations. (c) corresponding correlation plot of peak oxidation current (at 0.26 V) vs concentration of ferri/ferrocyanide. (d) An example CV taken during stability tests showing 1st to 3rd cyclic voltammograms (scan rate of 100 mV/s)acquired using a single Au-coated microelectrode in PBS (pH of 7.4).

 This work was supported by the Engineering and Physical Sciences Research Council under Grants numbers EP/R513143/1, EP/T517793/1, and EP/T025638/1.

REFERENCES

[1] S. Yu *et al.*, "A reconfigurable tri-mode frequency-locked loop readout circuit for biosensor interfaces," in *IEEE Transactions on Biomedical Circuits and Systems*, vol. 17, no. 4, 2023, pp. 768–781.

[2] M. Li, A. A. S. Gill, A. Vanhoestenberghe, and S. S. Ghoreishizadeh, "An integrated circuit for galvanostatic electrodeposition of on-chip electrochemical sensors," in *2022 29th IEEE International Conference on Electronics, Circuits and Systems (ICECS)*, 2022, pp. 1–4.

[3] H.-J. Kim *et al.*, "A dual-imaging speed-enhanced cmos image sensor for real-time edge image extraction," *IEEE Journal of Solid-State Circuits (JSSC)*, vol. 52, no. 9, pp. 2488–2497, 2017.

[4] B. Merriman, I. T. R&D Team, and J. M. Rothberg, "Progress in ion torrent semiconductor chip based sequencing," *Electrophoresis*, vol. 33, no. 23, pp. 3397–3417, 2012.

[5] N. Moser *et al.*, "Quantitative detection of dengue serotypes using a smartphone-connected handheld lab-on-chip platform," *Frontiers in Bioengineering and Biotechnology*, vol. 10, 2022.

[6] M. Carminati *et al.*, "Advances and open challenges for integrated circuits detecting bio-molecules," in *2018 25th IEEE International Conference on Electronics, Circuits and Systems (ICECS)*, 2018, pp. 857–860.

[7] W. Tedjo *et al.*, "Electrochemical biosensor system using a cmos microelectrode array provides high spatially and temporally resolved images," *Biosensors and Bioelectronics*, vol. 114, pp. 78–88, 2018.

[8] T. Xiao, J. Huang, D. Wang, T. Meng, and X. Yang, "Au and au-based nanomaterials: Synthesis and recent progress in electrochemical sensor applications," *Talanta*, vol. 206, p. 120210, 2020.

[9] R. Wrege *et al.*, "A cmos test chip with simple post-processing steps for dry characterization of isfet arrays," *IEEE Sensors Journal*, vol. 21, no. 4, 2021.

[10] J. Aziz, R. Genov *et al.*, "256-channel neural recording microsystem with on-chip 3d electrodes," in *2007 IEEE International Solid-State Circuits Conference. Digest of Technical Papers*, 2007, pp. 160–594.

[11] K. Niitsu *et al.*, "Development of microelectrode arrays using electroless plating for cmos-based direct counting of bacterial and hela cells," *IEEE Transactions on Biomedical Circuits and Systems*, vol. 9, no. 5, pp. 607–619, 2015.

[12] H. M. Jafari *et al.*, "Nanostructured cmos wireless ultra-wideband label-free pcr-free dna analysis soc," *IEEE JSSC*, vol. 49, no. 5, pp. 1223–1241, 2014.

[13] M. Datta, S. Merritt, and M. Dagenais, "Electroless remetallization of aluminum bond pads on cmos driver chip for flip-chip attachment to vertical cavity surface emitting lasers (vcsel's)," *IEEE Transactions on Components and Packaging Technologies*, vol. 22, no. 2, pp. 299–306, 1999.

[14] S. Hwang *et al.*, "Cmos microelectrode array for electrochemical lab-on-a-chip applications," *IEEE Sensors Journal*, vol. 9, no. 6, pp. 609–615, 2009.

[15] S. Choi *et al.*, "Methods of reducing non-specific adsorption in microfluidic biosensors," *Journal of Micromechanics and Microengineering*, vol. 20, no. 7, p. 075015, 2010.

[16] N. Saeidi *et al.*, "Technology for integrated circuit micropackages for neural interfaces, based on gold–silicon wafer bonding," *Journal of Micromechanics and Microengineering*, vol. 23, no. 7, p. 075021, jun 2013.

[17] K.-L. Lin and S.-Y. Chang, "The morphologies and the chemical states of the multiple zincating deposits on al pads of si chips," *Thin Solid Films*, vol. 288, no. 1, pp. 36–40, 1996.

[18] I. Othman *et al.*, "Impact of single and double zincating treatment on adhesion of electrodeposited nickel coating on aluminium alloy 7075," *Journal of Advanced Manufacturing Technology (JAMT)*, vol. 12, no. 1(3), pp. 179–192, 1 2018.

[19] D. Hutt, C. Liu, P. Conway, D. Whalley, and S. Mannan, "Electroless nickel bumping of aluminum bondpads. ii. electroless nickel plating," *IEEE Transactions on Components and Packaging Technologies*, vol. 25, no. 1, pp. 98–105, 2002.

[20] W. Shang *et al.*, "Deposition mechanism of electroless nickel plating of composite coatings on magnesium alloy," *Chemical Engineering Science*, vol. 207, 2019.

[21] O. Kasian *et al.*, "Electrochemical dissolution of gold in presence of chloride and bromide traces studied by on-line electrochemical inductively coupled plasma mass spectrometry," *Electrochimica acta*, vol. 222, 2016-12.